



**HAL**  
open science

## **Role of SiCl<sub>4</sub> addition in CH<sub>3</sub>F/O<sub>2</sub> based chemistry for Si<sub>3</sub>N<sub>4</sub> etching selectively to SiO<sub>2</sub>, SiCO and Si**

Francois Boulard, Valentin Bacquie, Aurelien Tavernier, Nicolas Posseme

### ► To cite this version:

Francois Boulard, Valentin Bacquie, Aurelien Tavernier, Nicolas Posseme. Role of SiCl<sub>4</sub> addition in CH<sub>3</sub>F/O<sub>2</sub> based chemistry for Si<sub>3</sub>N<sub>4</sub> etching selectively to SiO<sub>2</sub>, SiCO and Si. Journal of Vacuum Science & Technology A, 2023, 41 (3), pp.033002. 10.1116/6.0002434 . cea-04170423

**HAL Id: cea-04170423**

**<https://cea.hal.science/cea-04170423v1>**

Submitted on 25 Jul 2023

**HAL** is a multi-disciplinary open access archive for the deposit and dissemination of scientific research documents, whether they are published or not. The documents may come from teaching and research institutions in France or abroad, or from public or private research centers.

L'archive ouverte pluridisciplinaire **HAL**, est destinée au dépôt et à la diffusion de documents scientifiques de niveau recherche, publiés ou non, émanant des établissements d'enseignement et de recherche français ou étrangers, des laboratoires publics ou privés.

# Role of SiCl<sub>4</sub> addition in CH<sub>3</sub>F/O<sub>2</sub> based chemistry for Si<sub>3</sub>N<sub>4</sub> etching selectively to SiO<sub>2</sub>, SiCO and Si

François Boulard<sup>1,a</sup>, Valentin Bacquié<sup>1,b</sup>, Aurélien Tavernier<sup>1</sup>, and Nicolas Possémé<sup>1</sup>

<sup>1</sup> Univ. Grenoble Alpes, CEA, LETI, F-38000 Grenoble, France

- a) Author to whom correspondence should be addressed: [francois.boulard@cea.fr](mailto:francois.boulard@cea.fr)  
b) Current e-mail : [valentin.bacquie@st.com](mailto:valentin.bacquie@st.com)

Dry etching of amorphous silicon nitride (Si<sub>3</sub>N<sub>4</sub>) selectively toward silicon dioxide (SiO<sub>2</sub>), silicon oxycarbide (SiCO) and crystalline silicon (c-Si) in an Inductive Coupled Plasma (ICP) reactor using CHF<sub>3</sub>/O<sub>2</sub>/He chemistry with SiCl<sub>4</sub> addition is studied. Plasma exposure of c-Si, SiO<sub>2</sub> and SiCO leads to an oxifluoride deposition. The deposition rate is the same for all these materials and increases linearly with the amount of SiCl<sub>4</sub> added. On the other hand, Si<sub>3</sub>N<sub>4</sub> etching is observed at very small amount of SiCl<sub>4</sub> added (2 sccm) while oxide deposition takes place at higher SiCl<sub>4</sub> flow (10 sccm). Quasi-*in situ* Angle Resolved X-ray Photoelectron Spectroscopy (ARXPS) investigation shows oxifluoride SiO<sub>x</sub>F<sub>y</sub> deposition on c-Si and SiCO while a thin F-rich reactive layer is observed on Si<sub>3</sub>N<sub>4</sub>. The oxidation of Si<sub>3</sub>N<sub>4</sub> surface with O<sub>2</sub> plasma prior to CHF<sub>3</sub>/O<sub>2</sub>/He with small SiCl<sub>4</sub> addition plasma treatment showed that oxidation state plays a significant role on the etching / deposition equilibrium. In addition, it is found that oxifluoride deposition on Si<sub>3</sub>N<sub>4</sub> is driven by ion energy, with deposition observed at 0 V substrate bias voltage while etching is observed for values higher than to 150 V. All these results show that a competition takes place between silicon oxifluoride deposition and etching, depending on substrate material, surface oxidation and ion energy. Based on additional Optical Emission Spectroscopy (OES) data, we proposed insights to explain the different etching and deposition behaviors



This is the author's peer reviewed, accepted manuscript. However, the online version of record will be different from this version once it has been copyedited and typeset.  
PLEASE CITE THIS ARTICLE AS DOI: 10.1116/6.0002434

observed. It is focused on the crucial role of ion energy and the nitrogen presence in  $\text{Si}_3\text{N}_4$  leading to formation of CN and HCN, helping to get a thinner reactive layer and to evacuate etch by-products on  $\text{Si}_3\text{N}_4$  while an oxifluoride build-up on the other materials takes place.

## I. INTRODUCTION

The downscaling of Complementary Metal-Oxide-Semiconductor (CMOS) devices induces the need of significant process development at each new technology node in order to meet the aggressive specifications for 2D architectures on Fully Depleted Silicon On Insulator (FDSOI) and for 3D architectures as Fin Field Effect Transistor (FinFET)<sup>1</sup> or stacked nanowires (SNW)<sup>2</sup>. Independently of these transistor architectures, gate spacers have common interest. Their primary function is to electrically isolate the gate from the source and the drain and to define the effective channel length of the transistor by controlling the dopant profile<sup>3</sup>. Consequently, the spacer realization is critical regarding device performances. Gate spacers are commonly made of Si<sub>3</sub>N<sub>4</sub><sup>4</sup>. It tends to evolve to materials with lower dielectrics constant such as SiCOH<sup>5</sup> or SiBCN<sup>6</sup> in order to reduce RC delay. However, Si<sub>3</sub>N<sub>4</sub> spacers are still widely used at the lab or in the industry. Within the spacer module, the etching is particularly challenging for several reasons. First, spacers must be etched selectively toward the crystalline silicon (c-Si) constituting the source and the drain of the transistor and toward the silicon dioxide (SiO<sub>2</sub>) of the shallow trench isolation and/or the Buried OXide (BOX) of FDSOI technologies. Indeed, c-Si damage and c-Si/SiO<sub>2</sub> recesses are not suitable regarding device integration. In addition, it is important for the subsequent implantation module to preserve spacer Critical Dimensions (CDs) and to have straight profiles without foot formation at the base of the spacer. Finally, a new challenge appeared with 3D architectures. Because the active is lifted for these integrations, the apparition of parasitic spacer on its sidewalls with conventional etch need to be addressed by increasing significantly the over-etch time<sup>7</sup>. High selectivity etching

sequences are required to solve this specific issue in order to avoid significant recess into c-Si and SiO<sub>2</sub>.

Plasma etching of Si<sub>3</sub>N<sub>4</sub> for spacer application is mainly performed in ICP reactors using fluorocarbon C<sub>x</sub>F<sub>y</sub> or hydrofluorocarbon C<sub>x</sub>H<sub>y</sub>F<sub>z</sub>, like CF<sub>4</sub>, CHF<sub>3</sub> and CH<sub>3</sub>F<sup>8</sup>. The Si<sub>3</sub>N<sub>4</sub>/c-Si etch selectivity is increased by combining fluorocarbons with gases enhancing polymerization, such as dihydrogen (H<sub>2</sub>)<sup>9,10</sup> and methane (CH<sub>4</sub>)<sup>11</sup>. By reducing the fluorine radical concentration in the plasma through HF formation<sup>12</sup>, adding such gases leads to the formation of a carbon rich passivation layer C<sub>x</sub>F<sub>y</sub><sup>10</sup> preferentially on c-Si. However, this gas mixture might induce the formation of a large foot<sup>13</sup>, leading to a shift in dopant profile which could degrade CMOS transistor electrical performances. In addition, carbon-rich plasmas can also induce damages to the source and the drain by carbon implantation<sup>14</sup>. Dioxygen (O<sub>2</sub>) is usually added to these chemistries in order to have a precise control of the passivation layer thickness and to induce c-Si oxidation when landing on the active, enhancing selectivity<sup>8</sup>. Despite these optimizations, such etch processes do not meet all the requirements in terms of selectivity and profile control for 3D architectures spacer's, especially regarding the parasitic spacer removal mentioned above<sup>7</sup>.

Recent studies demonstrated the interest of adding silicon tetrachloride (SiCl<sub>4</sub>) to CH<sub>3</sub>F/O<sub>2</sub>/He chemistry<sup>13</sup>. Highly diluted SiCl<sub>4</sub> combined with significant O<sub>2</sub> flow induces a selective passivation layer deposition of SiO<sub>x</sub>F<sub>y</sub> over c-Si and SiO<sub>2</sub> while still etching Si<sub>3</sub>N<sub>4</sub>. Consequently, etch selectivity between these materials is significantly increased by SiCl<sub>4</sub> addition. As there is a significant SiO<sub>x</sub>F<sub>y</sub> deposition when landing on c-Si of the active, some oxide accumulation might occur around the active corner and prevent parasitic spacer etch removal on 3D architectures. Thus, the necessity to cycle the SiCl<sub>4</sub>-based etch

process with a carefully designed oxide etch step in order to overcome this issue has been demonstrated recently<sup>7</sup>, followed by process development and optimization of this etching sequence<sup>15</sup>. However, mechanisms of  $\text{SiO}_x\text{F}_y$  selective deposition on c-Si and  $\text{SiO}_2$  while  $\text{Si}_3\text{N}_4$  is etched remain unclear. The dependence of the initial growth kinetic on surface oxidation degree and thickness should be finely studied to take the full advantages of cyclic etch approaches.

In this paper, we first discuss the etching and deposition results on  $\text{Si}_3\text{N}_4$ , Si,  $\text{SiO}_2$  and SiCO as a function of  $\text{SiCl}_4$  flow. Reactive layer compositions are characterized by quasi *in situ* X-ray Photoelectron Spectroscopy (XPS) to clarify their compositions and thicknesses evolution. Then,  $\text{Si}_3\text{N}_4$  oxidation before etch and bias voltage are studied in order to highlight surface oxidation impact on etching and deposition mechanisms. These results are discussed to explain observed selectivity. Finally, OES signals are analyzed to highlight etching and deposition mechanisms.

## II. EXPERIMENTAL SETUP

### A. *Materials*

Thin films used in this study are deposited on 300 mm silicon blanket wafers or 16 nm thick Silicon On Insulator (SOI) wafers with 145 nm buried oxide.  $\text{Si}_3\text{N}_4$  with thicknesses of 53 or 140 nm are deposited by Low Pressure Chemical Vapor Deposition (LPCVD) at 750 °C from  $\text{SiH}_4$  and  $\text{NH}_3$  precursors. Thermally grown  $\text{SiO}_2$  and SiCO deposited by PEALD at 400 °C, both 100 nm thick, are also used.

### B. *Process conditions*

Etching or deposition experiments are conducted on 300 mm ICP Kiyoo FX etch module from LamResearch. Wafers are electrostatically clamped and chuck temperature is regulated thanks to backside He flow at 50 °C. Both source and chuck RF generators are operating at 13.56 MHz in continuous mode. All experiments in this study are conducted in bias voltage mode with continuous adjustment of bias RF power. CH<sub>3</sub>F/O<sub>2</sub>/He (200/200/120 sccm) with SiCl<sub>4</sub> addition ranging from 0 to 10 sccm gas mixtures are studied. Unless otherwise mentioned, plasma process conditions are 400 W for source power, 90 mtorr of total pressure, 60 s of exposure time and 250 V bias. Some experiments are conducted after thin films exposure to O<sub>2</sub>/He (200/220 sccm) plasma with 1000 W for source power, 10 mtorr of total pressure, 20 s of exposure time with 100 V or no bias applied to the substrate. Between experiments, the etch chamber is systematically cleaned and pre-coated in SiCl<sub>4</sub>/O<sub>2</sub> chemistry. Wet etching in hydrofluoric acid (HF) diluted to 1% in deionized water during 30 s is used prior (if mentioned) or after plasma exposure to remove native or deposited oxide, respectively.

### **C. Characterization setup**

Films thicknesses are characterized by ex-situ spectroscopic ellipsometry with wavelength ranging from 400 to 1000 nm on Atlas III from Nanometrics. All models include an oxide surface layer defined as a transparent film with thermal SiO<sub>2</sub> optical properties. This layer is used to describe native or plasma deposited oxide layers. Only films thicknesses are adjusted to experimental data.

Surface composition are carried out by quasi-*in situ* Angle Resolved X-ray Photoelectron Spectroscopy (ARXPS) measurements on a Thermo Fisher Scientific® Spectroscopy Theta300™ tool operating with a monochromatic Al K $\alpha$  x-ray source at

1486 eV. Wafers are transferred from etch to XPS chamber via a specific 300 mm compatible vacuum (pressure  $< 1 \times 10^{-4}$  mbar) carrier preventing from oxidation and airborne contamination<sup>16,17</sup>. Survey and narrow spectra are recorded with a pass energy of 100 eV and an energy step of 0.5 and 0.1 eV, respectively. A spot size of 400  $\mu\text{m}$  and 8 measurement angles, noted  $\theta$  in the following, from 23.75 to 76.25  $^\circ$  with respect to the surface normal are acquired. To limit surface charging, a flood gun is used, and the binding energy scale is referred to the adventitious C1s peak at 284.5 eV.

Optical Emission Spectroscopy (OES) measurements are achieved through OES plus setup provided by LamResearch. It covers a wavelength range from 185 to 983 nm with 2.0 nm spectral resolution and 100 ms integration time. The table reported by Piet.et.al<sup>18</sup> and references herein is used for the identification of H\* and O\* lines and CN\*, N<sub>2</sub>\* and NH\* bands. Signal from He\* at 587.7 nm is used to monitor the plasma electron density.

### III. RESULTS AND DISCUSSION

#### A. *Etch and deposition kinetics on Si<sub>3</sub>N<sub>4</sub>, Si, SiO<sub>2</sub> and SiCO*

Figure 1 shows the influence of SiCl<sub>4</sub> flow on oxide deposition rate on Si<sub>3</sub>N<sub>4</sub>, Si, SiO<sub>2</sub> and SiCO. Deposition rate are calculated from linear regression of deposition thickness versus plasma exposure time from 10 to 300 s. Deposition rates on Si, SiO<sub>2</sub> and SiCO increase linearly with the increasing of SiCl<sub>4</sub> flow from 2 to 10 sccm. They appear to be independent of the substrate material and reach  $0.45 \pm 0.01 \text{ nm} \cdot \text{s}^{-1}$  at 10 sccm of SiCl<sub>4</sub>. In contrary, a threshold is observed on Si<sub>3</sub>N<sub>4</sub> with no deposition at 2 sccm and deposition rate up to  $0.36 \text{ nm} \cdot \text{s}^{-1}$  at 10 sccm of SiCl<sub>4</sub>. In such condition, deposition rates remain 25 %

faster on Si, SiO<sub>2</sub> and SiCO than on Si<sub>3</sub>N<sub>4</sub>. It suggests that a competition between etch and deposition occurs on Si<sub>3</sub>N<sub>4</sub>. In the following, we focus on highly diluted SiCl<sub>4</sub> conditions with 2 sccm inlet flow, which presents a more contrasted sensitivity to materials. Kinetics of Si<sub>3</sub>N<sub>4</sub>, Si and SiCO films consumption are plotted on Figure 2 for plasma exposure from 10 to 300 s. Wet treatment by HF 1% during 30 s is applied before measurement in order to remove the deposited layer.

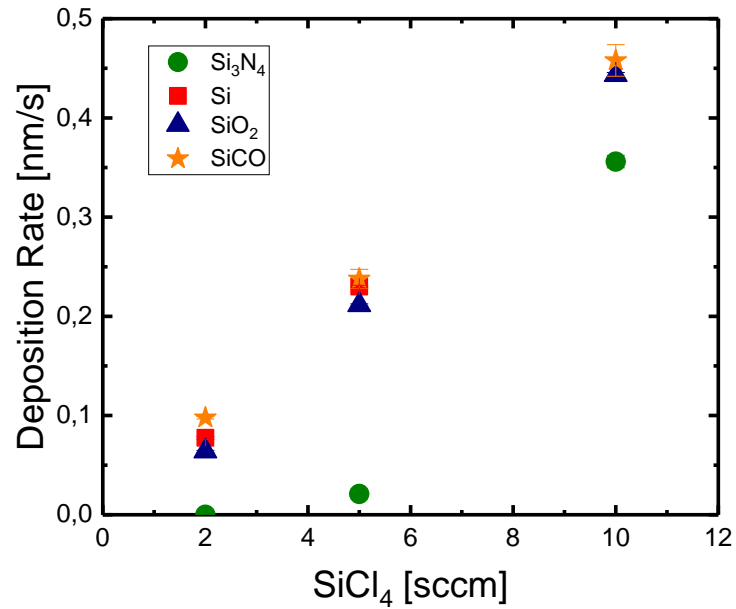


Figure 1: Dependence on SiCl<sub>4</sub> flow rate of overlayer deposition rate on Si<sub>3</sub>N<sub>4</sub>, Si, SiO<sub>2</sub> and SiCO.

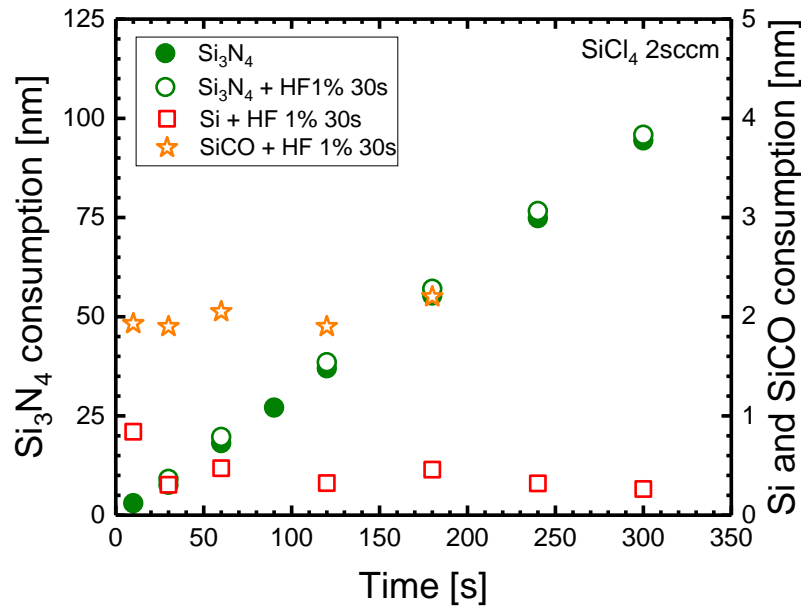


Figure 2: Si<sub>3</sub>N<sub>4</sub> (left axis), Si, and SiCO (right axis) consumption versus plasma exposure time for 2 sccm SiCl<sub>4</sub> flow rate. Measurements after HF 1% 30s treatment are presented by open symbols.

Si<sub>3</sub>N<sub>4</sub> consumption increases linearly with time, with an etch rate of 0.31 nm.s<sup>-1</sup>. The HF treatment leads to a constant increase of Si<sub>3</sub>N<sub>4</sub> consumption by a mean value of 1.6 nm. In contrast, Si and SiCO consumptions after plasma processes and HF treatment appear to be independent of plasma exposure time with values remaining below 1.0 and 2.2 nm on Si and SiCO, respectively. First, these observations show that HF 1% wet treatment efficiently removes the deposited silicon oxide at a rate higher than 0.66 nm.s<sup>-1</sup>. Second, it underlines that strongly diluted SiCl<sub>4</sub> conditions could lead to selective deposition on Si, SiO<sub>2</sub> and SiCO while Si<sub>3</sub>N<sub>4</sub> is etched. Finally, the 1.6 nm mean consumption induced by HF wet treatment post plasma exposure gives a first upper limit approximation of the reactive layer thickness.

To get insights into mechanisms and to figure out why deposition takes place on Si and SiCO films while Si<sub>3</sub>N<sub>4</sub> is etched, surface analysis after plasma exposure are performed by quasi *in-situ* XPS and compared to measurements on pristine films. Figure 3 presents Si2p high resolution spectra acquired at 23.75° relative to surface normal take-off angle on pristine SiCO, Si, and Si<sub>3</sub>N<sub>4</sub> and after plasma exposure of 30 and 60 s. After 30 s of plasma exposure, a peak at 104.0±0.5 eV attributed to Si-O bonds<sup>19</sup> appears on SiCO and Si while peaks at 102.7 and 99.2 eV attributed respectively to bulk Si-O-C<sup>20</sup> and Si-Si<sup>19</sup> contributions intensities decrease. This is even more pronounced after 60 s of plasma exposure. The attenuation of signals attributed to Si or SiCO bulk materials confirms the growth of a film containing silicon oxide on its top. At the opposite, on Si<sub>3</sub>N<sub>4</sub>, the ratio between peaks at 101.8 eV attributed to Si-N bonds<sup>21</sup> and at 103.5 eV attributed to Si-O bonds is not affected by plasma exposure. Si-N contribution dominates Si2p spectra independent of plasma exposure time. It suggests a steady etching of Si<sub>3</sub>N<sub>4</sub> film through the formation of a thin reactive surface layer, in accordance with kinetics results previously presented on Figure 2.

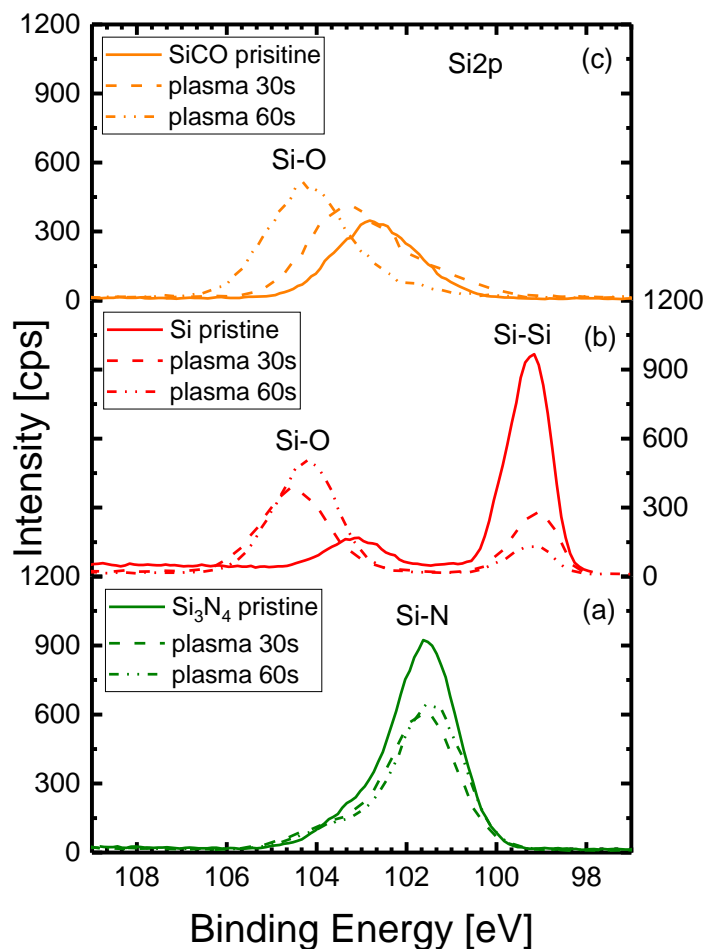


Figure 3 : Si2p high resolution spectra at  $23.75^\circ$  relative to surface normal take-off angle on Si<sub>3</sub>N<sub>4</sub> (a), Si (b), and SiCO (c) after 30 and 60 s of plasma exposure with 2 sccm SiCl<sub>2</sub> flow rate and vacuum transfer to XPS analysis chamber. Pristine films are measured ex-situ.

In addition, surface compositions are reported in Table 1. After 30 s of plasma exposure, silicon oxifluoride films deposited on Si and SiCO present stoichiometries of SiO<sub>1.8</sub>F<sub>0.9</sub> and SiO<sub>2.6</sub>F<sub>1.2</sub>, respectively. The deposit on SiCO appears O richer than on Si. However, O1s signal measured on SiCO could be partially attributed to bulk SiCO and not only oxifluoride deposit. Stoichiometries extracted from grazing angle measurements ( $\theta = 76.25^\circ$ ), with higher surface sensitivity, lead to SiO<sub>1.8</sub>F<sub>0.8</sub> on Si and SiO<sub>1.9</sub>F<sub>0.9</sub> on SiCO.

So, we can conclude that oxifluoride deposited on these films presents a similar composition. In contrast, plasma exposed  $\text{Si}_3\text{N}_4$  surface, which could be characterized by the ratio between Si bonded to N and N bonded to Si, presents a ratio of 0.78, which is very close to the ratio of 0.77 measured on pristine material. Main differences on  $\text{Si}_3\text{N}_4$  surface induced by the plasma exposure are the reduction of C and the presence of F-Si bonds. Surface contamination removal and reactive layer sensitivity allowed by quasi in-situ measurements could explain these observations.

Element (%)	Pristine films			After 30 s plasma exposure			After 70 s plasma exposure with $\text{O}_2$ plasma pre-treatment		
	$\text{Si}_3\text{N}_4$	Si	SiCO	$\text{Si}_3\text{N}_4$	Si	SiCO	With no bias $\text{Si}_3\text{N}_4$	With 100Vb $\text{Si}_3\text{N}_4$	
C1s	C-C	5.4	10.4	6.4	1.5	1.5	2.5	-	-
	C-O	1.4	2.0	-	-	-	-	-	-
	C=O	-	1.2	-	-	-	-	-	-
	C-Si	-	-	12.3	-	-	1.6	-	-
Cl2p	Cl-Cl	-	-	-	1.3	0.6	-	-	-
	F1s	0.6	-	-	11.7	21.5	20.6	11.7	24.5
O1s	O-Si	17.5	32.0	47.0	11.8	42.7	45.8	14.2	43.8
N1s	N-Si	38.2	-	-	38.0	-	-	38.0	2.2
	Si-O	7.6	9.0	20.9	6.2	24.1	17.4	7.1	26.6
Si2p	Si-N	29.3	-	-	29.6	-	-	29.0	2.8
	Si-C	-	-	13.4	-	-	12.1	-	-
	Si-Si	-	45.5	-	-	10.6	-	-	-

Table 1 : Surface composition measured by quasi in-situ XPS ( $\theta = 23.75^\circ$ ) on Si, SiCO, and  $\text{Si}_3\text{N}_4$  before and after plasma exposure. Pristine films are measured ex-situ. Measurements with additional  $\text{O}_2$  plasma pre-treatment are also reported.

Table 1 also reports few % of chlorine after plasma exposure on surfaces of  $\text{Si}_3\text{N}_4$  and Si films. Chlorine is also observed on SiCO for shorter 10 s plasma exposure and on Si sample for longer 120 s experiments. These values, ranging from 0 to 1.3 %, are close to the detection limits of the experimental conditions used in this study. Figure 4 plots Cl2p

This is the author's peer reviewed, accepted manuscript. However, the online version of record will be different from this version once it has been copyedited and typeset.  
PLEASE CITE THIS ARTICLE AS DOI: 10.1116/1.5002434

and F1s surface compositions measured on Si<sub>3</sub>N<sub>4</sub>, Si, and SiCO samples as a function of plasma exposure time for a much more surface sensitive condition ( $\theta = 76.25^\circ$ ). On Si<sub>3</sub>N<sub>4</sub> sample, chlorine continuously decreases from 3.5 % after 10 s of plasma exposure until 0 % after 240 s. Fluorine surface composition ranges between 20.5 and 22.4 % and appears independent of process duration. As suggested by Ullal et.al.<sup>22,23</sup> and Kogelschatz et.al.<sup>24</sup>, these observations could be interpreted as the replacement of Si-Cl by Si-F bonds at the surface. However, in our conditions, SiO<sub>x</sub>Cl<sub>y</sub>F<sub>z</sub> deposition is not observed on Si<sub>3</sub>N<sub>4</sub> with 2 sccm of SiCl<sub>4</sub>. Plasma exposure are systematically achieved after a chamber conditioning with a wall coating with SiO<sub>x</sub>Cl<sub>y</sub> film. Surface analysis have been performed on Si<sub>3</sub>N<sub>4</sub> after 60 s of plasma exposure without coating deposition during the conditioning sequence. No Cl2p was detected in such conditions. Consequently, we attribute Cl2p signals reported in Table 1 and Figure 4 to the wall coating etching, which probably takes place in the high plasma density region of the reactor close to the powered antenna.

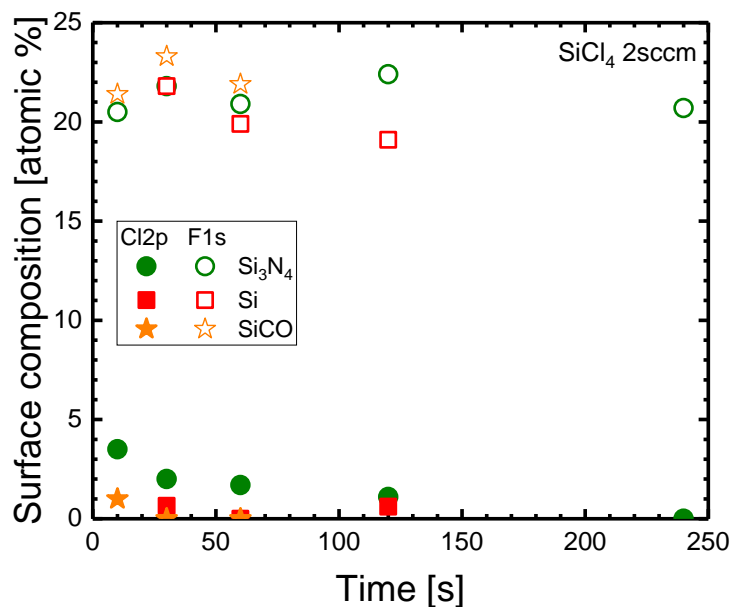


Figure 4 : Quasi in-situ XPS ( $\theta = 76.25^\circ$ ) Cl2p and F1s atomic % measured on Si<sub>3</sub>N<sub>4</sub> (green dot), Si (red square), and SiCO (orange star) in function of plasma exposure time.

At this point, highly diluted SiCl<sub>4</sub> (2 sccm) addition in CH<sub>3</sub>F/O<sub>2</sub>/He (200/200/120 sccm) plasma operated at 90 mtorr with source power of 400 W and 250 V bias voltage etches Si<sub>3</sub>N<sub>4</sub> at a constant rate of 0.31 nm.s<sup>-1</sup> through a thin (< 1.6 nm) F-rich reactive layer. The same process condition leads to SiO<sub>1.8</sub>F<sub>0.8</sub> deposition on Si or SiCO with deposition rate in the range of 0.06 to 0.10 nm.s<sup>-1</sup>. Chlorine is attributed to the chamber conditioning scheme and not to the plasma etch/deposition process itself.

### B. Influence of Si<sub>3</sub>N<sub>4</sub> oxidation

To figure out why in our conditions Si<sub>3</sub>N<sub>4</sub> is etched while Si, SiO<sub>2</sub>, and SiCO surfaces lead to the growth of an oxifluoride layer, the oxidation of Si<sub>3</sub>N<sub>4</sub> surface by O<sub>2</sub> plasma and its impact on etch or deposition is explored. Figure 5 presents Si2p spectra

evolution with take-off angle for pristine Si<sub>3</sub>N<sub>4</sub> (a) and after exposure to O<sub>2</sub> plasma during 20 s with no bias (b) or with 100 V bias (c) applied on the substrate. On pristine Si<sub>3</sub>N<sub>4</sub>, whatever the angle, contribution attributed to Si-N bonds is more intense than the one of Si-O bonds. At grazing angle, both contributions tend toward a similar intensity. These variations could be interpreted as the presence of a thin oxidized surface layer on top of pristine Si<sub>3</sub>N<sub>4</sub>. After O<sub>2</sub> plasma, Si-O contribution is more intense and Si-O to Si-N area ratio grows with the increase of the take-off angle. These tendencies are even more pronounced with 100 V bias voltage applied to the substrate. It suggests that O<sub>2</sub> plasma treatment induces a thicker oxidized surface layer. Its thickness increases with the use of bias voltage. We use the method first introduced by Carlson and McGuire<sup>25</sup> to estimate the over-layer oxide thickness. We exclude 69 and 76° grazing angle data and we use a constant 1.2 eV chemical shift between Si-N and Si-O<sup>26</sup> in the fitting procedure. We assume a similar inelastic mean free path of 3.5 nm for electron escaping Si<sub>3</sub>N<sub>4</sub> or SiO<sub>2</sub> and use by simplification an intensity ratio of 1 between bulk Si<sub>3</sub>N<sub>4</sub> and SiO<sub>2</sub>. Under these assumptions, fitting the evolution of Si-O to Si-N area ratio with the reverse of the take-off angle cosine leads to oxide over-layer thickness of 0.7, 1.7, and 2.2 nm for pristine Si<sub>3</sub>N<sub>4</sub>, after O<sub>2</sub> plasma with no applied bias, and after O<sub>2</sub> plasma with 100 V applied bias, respectively.

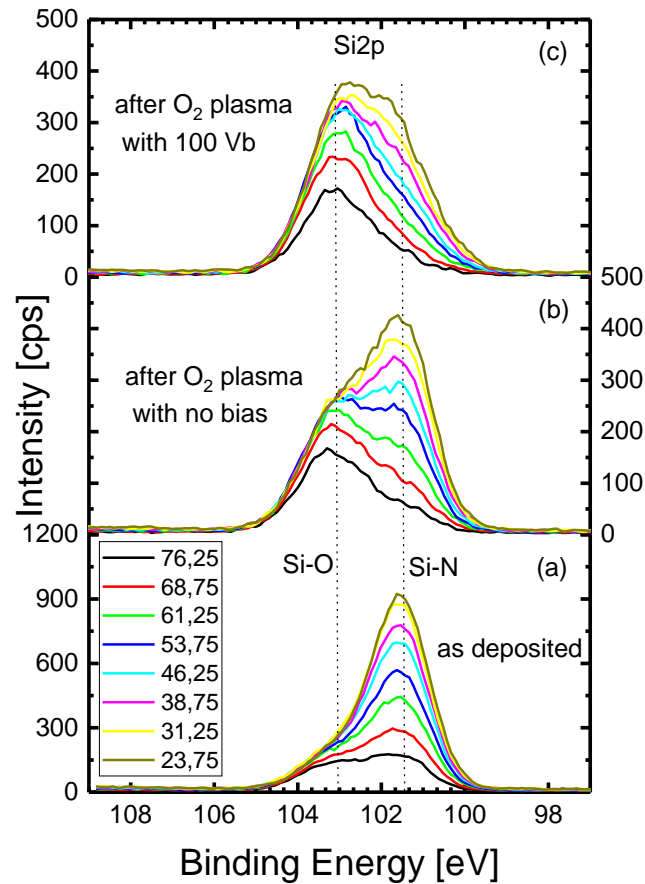


Figure 5 : Take-off angle relative to surface normal dependence of Si2p high-resolution spectra measured on as deposited Si<sub>3</sub>N<sub>4</sub> (a) and after O<sub>2</sub> plasma treatment with no bias (b) or 100 Vb (c).

The impact of these surface states on the ability to etch Si<sub>3</sub>N<sub>4</sub> in highly diluted SiCl<sub>4</sub> is studied. As discussed in section A, without deliberate oxidation, a Si<sub>3</sub>N<sub>4</sub> consumption of 18.1 nm is observed after 60 s of plasma exposure. When O<sub>2</sub> plasma is performed without bias, this value is reduced to 7.0 nm. Finally, on surface treated by O<sub>2</sub> plasma with 100 V bias, which presents a thicker oxide layer, no consumption but a 1.8 nm deposit is measured. Corresponding surface compositions are reported in Table 1. Surface compositions after SiCl<sub>4</sub> based plasma exposure are very similar for surfaces pre-oxidized

by O<sub>2</sub> plasma with or without bias. Only a small difference is observed. Compared to pristine Si<sub>3</sub>N<sub>4</sub>, wafer with O<sub>2</sub> plasma pre-treatment presents an increase of Si-O and O-Si contributions of 0.9 and 2.4 %, respectively. It indicates a slightly more oxidized surface on wafer with O<sub>2</sub> pre-treatment than on pristine Si<sub>3</sub>N<sub>4</sub>. It could explain the drop of Si<sub>3</sub>N<sub>4</sub> consumption from 18 to 7 nm by the displacement of the etch/deposition equilibrium toward more deposition promoted by a thicker surface oxide layer. This interpretation is reinforced by the surface composition of the most pre-oxidized case, which indicates the presence of SiO<sub>1.5</sub>F<sub>0.9</sub> on top of Si<sub>3</sub>N<sub>4</sub> when SiCl<sub>4</sub> based plasma exposure is used on surface pre-treated by O<sub>2</sub> plasma with 100 V bias. These results point out the influence of the Si<sub>3</sub>N<sub>4</sub> surface oxide thickness on the etch/deposition equilibrium with a switch toward etching when the initial oxide thickness is thinner than 1.7 nm. At the opposite, O<sub>2</sub> plasma with 100 V bias voltage forms an oxidized surface layer sufficiently thick to stop the Si<sub>3</sub>N<sub>4</sub> etching and leads to oxifluoride deposition. Note that in these conditions, the deposition rate on Si<sub>3</sub>N<sub>4</sub> remains 2 to 3 times lower than on Si and SiCO. Why etching occurs in highly oxidized plasma under 250 V bias voltage? How the equilibrium between reactive layer thickness, oxide formation, and etching is modified by bias voltage? Next section explores these questions of the influence of substrate bias voltage on Si<sub>3</sub>N<sub>4</sub> etching.

### **C. Role of ion energy**

Figure 6 presents the influence of substrate bias voltage on the Si<sub>3</sub>N<sub>4</sub> consumption thickness or overlayer oxide deposition thickness after 60 s of plasma processing. These experiments are performed on HF last films in order to limit the impact of native oxide. Quasi *in-situ* XPS Si2p high resolution spectra acquired after plasma processing at 0 (black), 150 (red) and 250 V (green) bias voltage as well as a reference Si<sub>3</sub>N<sub>4</sub> film freshly

treated by HF (dashed black line) are shown in the Figure 6 inset. These spectra are normalized to the peak at 101.8 eV attributed to Si-N contribution, stressing the impact of the process on Si-O environment at higher binding energy. With 0 V bias applied on the substrate, Si<sub>3</sub>N<sub>4</sub> is not consumed and a 3.0 nm oxide overlayer is measured. This is consistent with the Si-O to Si-N ratio larger than 1 which is observed on associated Si2p spectra. When the bias voltage increases, a transition between deposition and etching occurs. Such transition is also clearly visible on Si2p spectra where Si-O contribution strongly decreases in favor of Si-N environment. However, in comparison with HF last Si<sub>3</sub>N<sub>4</sub> surface, Si2p spectra measured after plasma processing with 250 V bias voltage still presents a shoulder on its high energy side. We attribute such shoulder to the reactive layer on top of bulk Si<sub>3</sub>N<sub>4</sub>. Its relative intensity decreases with the bias voltage increasing, suggesting that in the etching regime, the reactive layer thickness is thinned by the etch products removal. In pure O<sub>2</sub> plasma, which are not suited to etch Si<sub>3</sub>N<sub>4</sub>, previous results showed that the oxide thickness formed on top of Si<sub>3</sub>N<sub>4</sub> increases with the rise of ion bombardment energy. In CH<sub>3</sub>F/O<sub>2</sub>/He (200/200/120 sccm) plasma chemistry with 2 sccm of SiCl<sub>4</sub>, the ion energy increase leads to a rise of the etch rate and a thinning of the reactive layer thickness.

Comparable experiments are conducted on Si. Without bias voltage applied to the substrate, a 3.1 nm thick oxide overlayer is observed. This value is similar to the one measured on Si<sub>3</sub>N<sub>4</sub>. By contrast, the rise of the bias voltage from 0 to 350 V conducts to an increase of the oxide overlayer from 3.1 to 4.8 nm. Measurement of the Si film thickness after oxide removal by HF wet treatment indicates that the Si consumption remains below 1.0 nm, even for the more energetic condition with 350 V bias voltage.

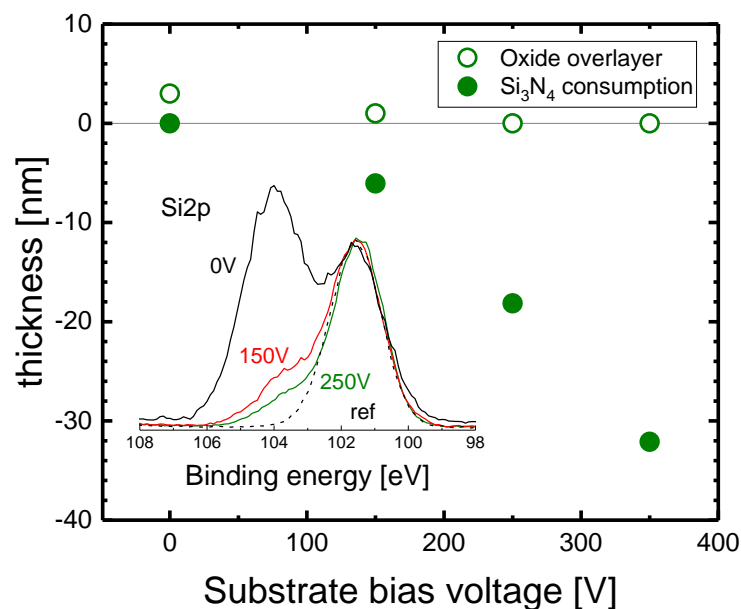


Figure 6 : Influence of substrate bias voltage on Si<sub>3</sub>N<sub>4</sub> consumption (full dot) or oxide overlayer (open dot) thicknesses. Plasma duration is 60 s. Si<sub>3</sub>N<sub>4</sub> films are deoxidized in HF 1% during 60 s prior running plasma experiments. Inset presents XPS high resolution spectra ( $\theta = 23.75^\circ$ ) of Si2p before (black dashed line) and after plasma processing with 0 V (black), 150 V (red), and 250 V (green) bias voltage.

#### D. Discussion

To sum up, relatively high bias voltage of 250 V and the use of an oxidizing chemistry with the addition of a small amount of SiCl<sub>4</sub> (<0.4% of the total flow) leads to the deposition of silicon oxifluoride layer on Si, SiCO, and SiO<sub>2</sub> materials. The deposition rate increases linearly with the rise of SiCl<sub>4</sub> flow from 2 to 10 sccm. On Si<sub>3</sub>N<sub>4</sub>, deposition is also observed when the surface presents an oxidized overlayer thicker than 2.2 nm. It turns toward etching if the oxidized layer is thinner than 1.7 nm. The etch rate decreases with the bias voltage reduction until silicon oxifluoride deposition dominates at 0 bias voltage, even on deoxidized HF last Si<sub>3</sub>N<sub>4</sub> surface. These results show that a competition takes place between silicon oxifluoride deposition and Si<sub>3</sub>N<sub>4</sub> etching. The equilibrium

depends on substrate material, surface oxide layer thickness, and ions bombardment energy.

Oxychloride deposition on chamber wall have been studied in  $\text{Cl}_2/\text{O}_2$ <sup>22</sup> or  $\text{HBr}/\text{Cl}_2/\text{O}_2$ <sup>24</sup> chemistries used in Si gate or trench patterning. These studies suggest that silicon oxychloride is deposited through oxidation of  $\text{SiCl}_x$  molecules adsorbed on chamber wall<sup>22</sup> and that the film composition is not constant through its thickness<sup>24</sup>. The deposited layer could be etched in F-rich  $\text{SF}_6$  chemistry through film fluorination by abstraction<sup>23</sup> or substitution<sup>24</sup> of Cl by F atoms, leading to silicon oxyfluoride film.

What is specific to  $\text{Si}_3\text{N}_4$  in comparison of Si,  $\text{SiO}_2$  or  $\text{SiCO}$  to explain that etching is favored over silicon oxifluoride deposition? The larger Si-O ( $800 \text{ kJ}\cdot\text{mol}^{-1}$ ) than Si-N ( $437 \text{ kJ}\cdot\text{mol}^{-1}$ ) bond energy<sup>27</sup> is sometimes assumed as the cause of etch selectivity<sup>15,21,28</sup>. However, published data present some discrepancies with bond energy of Si-O close to the bond energy of Si-N ( $368$  and  $335 \text{ kJ}\cdot\text{mol}^{-1}$ , respectively<sup>29</sup>). Bond energy or strength is defined as the enthalpy of dissociation of diatomic molecules in gaseous state. Its relevance to explain plasma surface interaction is questionable. In order to progress, we analyze the OES acquired during the etching of 53 nm thick  $\text{Si}_3\text{N}_4$  layer deposited on 10 nm thick  $\text{SiO}_2$  on Si. According to  $\text{Si}_3\text{N}_4$  consumption kinetics presented above, 170 s are needed to remove the layer before landing on  $\text{SiO}_2$ . On Figure 7 is plotted the difference of optical spectra acquired at 180 and 140 s, i.e. after landing on  $\text{SiO}_2$  and during  $\text{Si}_3\text{N}_4$  etching, respectively. Such representation highlights substrate material sensitive lines, with negative (positive) intensities attributed to decreasing (increasing) lines when the transition from  $\text{Si}_3\text{N}_4$  etching to deposition on  $\text{SiO}_2$  takes place. Species are attributed to the wavelengths as reported by Piet et al<sup>18</sup>, the transition from  $\text{Si}_3\text{N}_4$  etching to deposition on

This is the author's peer reviewed, accepted manuscript. However, the online version of record will be different from this version once it has been copyedited and typeset.  
PLEASE CITE THIS ARTICLE AS DOI: 10.1116/1.6.0002434

SiO<sub>2</sub> leads to the reduction of NH, N<sub>2</sub> and CN lines intensities while lines attributed to O and H increase.

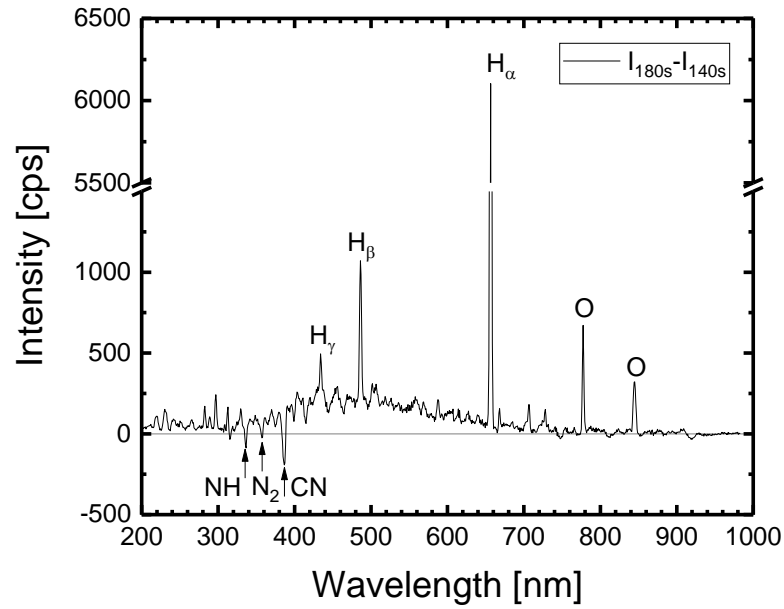


Figure 7 : Difference of optical emission spectra acquired at 140 and 180 s during plasma processing of a 53 nm thick Si<sub>3</sub>N<sub>4</sub> on 10 nm SiO<sub>2</sub> on Si wafer. The Si<sub>3</sub>N<sub>4</sub> layer is expected to be fully etched after 170 s.

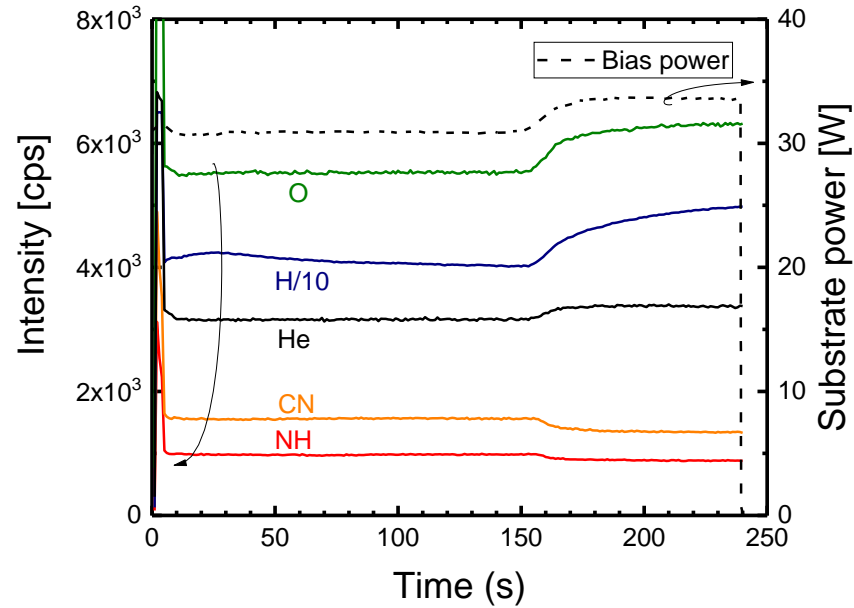


Figure 8 : Time dependence of NH, CN, He, H (divided by 10) and O optical lines intensities (left axis) and substrate power applied to the wafer for 250 bias voltage (right axis) during plasma processing of a 53 nm thick  $\text{Si}_3\text{N}_4$  on 10 nm  $\text{SiO}_2$  on Si wafer.

The time evolution of these lines and the substrate power required to maintain 250 bias voltage are plotted on Figure 8. First seconds exhibit strong variations attributed to the plasma strike. Then, signals do not vary until a transition appears between 155 and 175 s. It confirms previous kinetics results expecting the end of  $\text{Si}_3\text{N}_4$  etching at 170 s. Above all, these results give interesting insight to improve the understanding of  $\text{Si}_3\text{N}_4$  etching mechanisms and its selectivity to  $\text{SiO}_2$ . The decrease of CN and NH lines intensities at the end of  $\text{Si}_3\text{N}_4$  removal indicates that the formation of these species is a path to remove N from  $\text{Si}_3\text{N}_4$ . Consequently, it suggests that C and H are consumed during  $\text{Si}_3\text{N}_4$  etching. In addition, volatile NO could be formed but no clear evidence were found in our data. The increase of H and O when silicon oxifluoride takes place on  $\text{SiO}_2$  could be interpreted as the ending of H and O radicals consumption by reactions with N and CN to form volatiles

NH, NO, and HCN by-products. Note that the rise of these line intensities are also partially due to a plasma density increase as indicated by the larger bias power needed to maintain 250 bias voltage. However, such increase is still present after normalization by the intensity of He line at 587.7 nm, meaning that it also denotes a specie density increase. These observations highlight the role of N by formation of CN which could react with H to form volatile HCN species<sup>30,31</sup> and remove the reactive polymer surface layer. Classically, in fluorocarbon based chemistry, SiO<sub>2</sub> etching and its selectivity to Si invokes the role of O as a polymer inhibitor associated to CO or CO<sub>2</sub> formation. Here, in presence of SiCl<sub>4</sub>, we have seen that oxidized surfaces favors the growth of an oxifluoride layer, which should take the lead over polymer layer removal. On Si<sub>3</sub>N<sub>4</sub> surface, with sufficient bias power applied to the substrate, our experimental results and interpretations suggest that the Si<sub>3</sub>N<sub>4</sub> etching selectivity over Si, SiO<sub>2</sub> or SiCO could be attributed to the formation of CN etch products which limits reactive layer thickness and allow a steady removal of etch products.

#### IV. CONCLUSION.

The addition of small amount of SiCl<sub>4</sub> to CH<sub>3</sub>F/O<sub>2</sub>/He plasma on Si<sub>3</sub>N<sub>4</sub>, c-Si, SiO<sub>2</sub> and SiCO etching and oxide overlayer deposition has been investigated. A strong correlation is observed between the amount of SiCl<sub>4</sub> added to the plasma and the oxifluoride deposition rate on all materials. If deposition occurs systematically on Si, SiO<sub>2</sub> and SiCO even at low SiCl<sub>4</sub> flow, on Si<sub>3</sub>N<sub>4</sub> the amount of SiCl<sub>4</sub> added controls at the first order the etching (low SiCl<sub>4</sub> flow) or the deposition (high SiCl<sub>4</sub> flow) behavior. Depending if the Si<sub>3</sub>N<sub>4</sub> surface is slightly or strongly oxidized, a significant etch slowdown or the deposition of a thin oxifluoride is observed, respectively. It strongly indicates that

oxidation state is a major  $\text{Si}_3\text{N}_4$  etch inhibitor using  $\text{CH}_3\text{F}/\text{O}_2/\text{He}/\text{SiCl}_4$  chemistry and it is consistent with the deposition behavior previously observed on other silicon-based oxidized materials, such as  $\text{SiO}_2$  and  $\text{SiCO}$ . In addition, oxifluoride deposition occurs on  $\text{Si}_3\text{N}_4$  at no or low bias voltage applied to the substrate. Such deposition quickly decreases when bias voltage increases until  $\text{Si}_3\text{N}_4$  is etched for high bias voltage (150 V or more), indicating that there is an ion energy threshold switching the equilibrium from deposition to etch. On the other side, oxifluoride deposition on c-Si increases with bias voltage suggesting that, beyond oxidation state and ion energy threshold,  $\text{Si}_3\text{N}_4$  has some particularity compared to the other materials studied leading to a specific behavior when exposed to  $\text{CH}_3\text{F}/\text{O}_2/\text{He}/\text{SiCl}_4$ . The use of OES during  $\text{Si}_3\text{N}_4$  etching highlights that C and H from plasma gas feed are mainly consumed through NH, CN and HCN by-products formation. We believe that the volatile by-products formation on  $\text{Si}_3\text{N}_4$  under the right process condition (ie, sufficient bias voltage) is the key differentiator to limit reactive layer thickness and to allow a steady etch while deposition occurs on the other materials.

## AUTHOR DECLARATIONS

### Conflict of interest

The authors have no conflicts to disclose.

### Authors Contribution

**François Boulard** : Writing – original draft (equal), Writing – review & editing (lead), Formal analysis (supporting), Validation (equal), Supervision (supporting)

**Valentin Bacquié** : Writing – original draft (equal), Writing – review & editing (supporting), Investigation, Conceptualization (equal), Formal analysis (lead), Resources,



**Aurélien Tavernier** : Writing-original draft (equal), Writing – review & editing (supporting), Conceptualization (equal), Validation (equal), Supervision (supporting)

**Nicolas Posseme** : Funding acquisition, Conceptualization (equal), Writing – review & editing (supporting), Project administration, Supervision (lead)

## DATA AVAILABILITY

The data that support the findings of this study are available upon reasonable request.

## REFERENCES

- <sup>1</sup>R. Xie *et al.*, 2016 IEEE International Electron Devices Meeting (IEDM), San Francisco, CA, 3-7 December 2016 (IEEE, 2016), pp 16.47-16.50
- <sup>2</sup>S. Barraud *et al.*, 2017 IEEE International Electron Devices Meeting (IEDM), San Francisco, CA, 2-6 December 2017 (IEEE, 2017), pp 17.677-17.680
- <sup>3</sup>R. A. Gottscho, K. Nojiri, and J. LaCara, *Thin Solid Films* **516**, 3493 (2008).
- <sup>4</sup>F. Koehler, D. Triyoso, I. Hussain, S. Mutas, and H. Bernhardt, *IOP Conf. Ser. Mater. Sci. Eng.* **41**, 012006 (2012).
- <sup>5</sup>E. Huang *et al.*, "Low-k Spacers for Advanced Low Power CMOS Devices with Reduced Parasitic Capacitances", 2008 IEEE International SOI Conference Proceedings (IEEE, 2008), pp 19-20.
- <sup>6</sup>R. Divakaruni and V. Narayanan, *ECS Trans.* **72**, 3 (2016).
- <sup>7</sup>O. Pollet, V. Ah-Leung, S. Barnola, and N. Posseme, *J. Vac. Sci. Technol., A* **38**, 063007 (2020).
- <sup>8</sup>R. Blanc, F. Leverd, T. David, and O. Joubert, *J. Vac. Sci. Technol. B* **31**, 051801 (2013).

- <sup>9</sup>J. W. Coburn, J. Appl. Phys. **50**, 5210 (1979).
- <sup>10</sup>G. S. Oehrlein and H. L. Williams, J. Appl. Phys. **62**, 662 (1987).
- <sup>11</sup>S. Lee, J. Oh, K. Lee, and H. Sohn, J. Vac. Sci. Technol. B **28**, 131 (2010).
- <sup>12</sup>T. C. Mele, J. Nulman, and J. P. Krusius, J. Vac. Sci. Technol., B **2**, 684 (1984).
- <sup>13</sup>N. Possémé, M. Garcia-Barros, C. Arvet, O. Pollet, F. Leverd, and S. Barnola, J. Vac. Sci. Technol. A **38**, 033004 (2020).
- <sup>14</sup>R. Blanc, M. Darnon, G. Cunge, S. David, F. Leverd, and O. Joubert, J. Vac. Sci. Technol. B **32**, 021806 (2014).
- <sup>15</sup>V. Bacquié, A. Tavernier, F. Boulard, O. Pollet, and N. Possémé, J. Vac. Sci. Technol. A. **39**, 033005 (2021)
- <sup>16</sup>B. Pelissier, H. Kambara, E. Godot, E. Veran, V. Loup, and O. Joubert, Microelectron. Eng. **85** (2008), pp 151–155.
- <sup>17</sup>B. Pelissier, S. Labau, M. Martin, C. Petit-Etienne, H. Fontaine, T. Baron, and O. Joubert, Microelectron. Eng. **231**, 111401 (2020).
- <sup>18</sup>J. Piet, W. Faider, A. Girard, F. Boulard, and C. Cardinaud, J. Vac. Sci. Technol. A **38**, 053005 (2020).
- <sup>19</sup>J.F. Moulder, W.F. Stickle, P.E. Sobol, and K.D. Bomben, Handbook of X-Ray Photoelectron Spectroscopy, PerkinElmer, Eden Prairie, (1992).
- <sup>20</sup>A. Avila, I. Montero, L. Galan, J.M. Ripalda, and R. Levy, J. Appl. Phys. **89**, 212, (2001).
- <sup>21</sup>M. Schaepkens, T.E.F.M. Standaert, N. R. Rueger, P.G.M. Sebel, G.S. Oehrlein, and J.M. Cook, J. Vac. Sci. Technol. A **17**, 26 (1999).

This is the author's peer reviewed, accepted manuscript. However, the online version of record will be different from this version once it has been copyedited and typeset.  
PLEASE CITE THIS ARTICLE AS DOI: 10.1116/6.0002434

- <sup>22</sup>S.J. Ullal, H. Singh, V. Vahedi, and E.S. Aydil, *J. Vac. Sci. Technol., A* **20**(2), (2002), pp 499-506.
- <sup>23</sup>S.J. Ullal, H. Singh, J. Daugherty, V. Vahedi, and E.S. Aydil, *J. Vac. Sci. Technol. A* **20**, 1195 (2002).
- <sup>24</sup>M. Kogelschatz, G. Cunge, and N. Sadeghi, *J. Vac. Sci. Technol. A* **22**, 624 (2004).
- <sup>25</sup>T.A. Carlson, G.E. McGuire, *J. Electron. Spectrosc.* **1**, (1972/73).
- <sup>26</sup>E. Ravizza, S. Spadoni, R. Piagge, P. Comite, and C. Wiemer, *Surf. Interface Anal.* **44**, 1209-1213 (2012).
- <sup>27</sup>D. R. Lide, "Strengths of Chemical Bonds", in *CRC Handbook of Chemistry and Physics, Internet Version 2005*, ed., <<http://www.hbcnpnetbase.com>>, CRC Press, Boca Raton, FL, (2005).
- <sup>28</sup>L. Chen, L. Xu, D. Li and B. Lin, *Microelectron. Eng.* **86** (11), (2009), pp 2354-2357.
- <sup>29</sup>F.A. Cotton, G. Wilkinson, *Advanced Inorganic Chemistry A comprehensive text*, Third Edition, Interscience Publishers, 1972
- <sup>30</sup>C.K. Park, H.T. Kim, C.H. Lee, N.E. Lee, and H; Mok, *Microelectron. Eng.* **85** (2), (2008) pp 375-387.
- <sup>31</sup>T. Ito, K. Karahashi, M. Fukasawa, T. Tatsumi, and S. Hamaguchi, *J. Vac. Sci. Technol. A* **29**, 050601 (2011).

## TABLES

Element (%)	Pristine films			After 30 s plasma exposure			After 70 s plasma exposure with O <sub>2</sub> plasma pre-treatment	
	Si <sub>3</sub> N <sub>4</sub>	Si	SiCO	Si <sub>3</sub> N <sub>4</sub>	Si	SiCO	With no	With
							bias	100Vb
	Si <sub>3</sub> N <sub>4</sub>	Si	SiCO	Si <sub>3</sub> N <sub>4</sub>	Si	SiCO	Si <sub>3</sub> N <sub>4</sub>	Si <sub>3</sub> N <sub>4</sub>
C-C	5.4	10.4	6.4	1.5	1.5	2.5	-	-
C1s	C-O	1.4	2.0	-	-	-	-	-
	C=O	-	1.2	-	-	-	-	-
	C-Si	-	-	12.3	-	-	1.6	-
Cl2p	Cl-Cl	-	-	-	1.3	0.6	-	-
	F1s	0.6	-	-	11.7	21.5	20.6	11.7
O1s	O-Si	17.5	32.0	47.0	11.8	42.7	45.8	14.2
N1s	N-Si	38.2	-	-	38.0	-	-	38.0
	Si-O	7.6	9.0	20.9	6.2	24.1	17.4	7.1
Si2p	Si-N	29.3	-	-	29.6	-	-	29.0
	Si-C	-	-	13.4	-	-	12.1	-
	Si-Si	-	45.5	-	-	10.6	-	-

Table 1 : Surface composition measured by quasi in-situ XPS ( $\theta = 23.75^\circ$ ) on Si, SiCO, and Si<sub>3</sub>N<sub>4</sub> before and after plasma exposure. Pristine films are measured ex-situ. Measurements with additional O<sub>2</sub> plasma pre-treatment are also reported.



## FIGURE CAPTIONS

Figure 1 : Dependence on SiCl<sub>4</sub> flow rate of overlayer deposition rate on Si<sub>3</sub>N<sub>4</sub>, Si, SiO<sub>2</sub> and SiCO.

Figure 2 : Si<sub>3</sub>N<sub>4</sub> (left axis), Si, and SiCO (right axis) consumption versus plasma exposure time for 2 sccm SiCl<sub>4</sub> flow rate. Measurements after HF 1% 30s treatment are presented by open symbols.

Figure 3 : Si2p high resolution spectra at 23.75° relative to surface normal take-off angle on Si<sub>3</sub>N<sub>4</sub> (a), Si (b), and SiCO (c) after 30 and 60 s of plasma exposure with 2 sccm SiCl<sub>2</sub> flow rate and vacuum transfer to XPS analysis chamber. Pristine films are measured ex-situ.

Figure 4 : Quasi in-situ XPS ( $\theta = 76.25^\circ$ ) Cl2p and F1s atomic % measured on Si<sub>3</sub>N<sub>4</sub> (green dot), Si (red square), and SiCO (orange star) in function of plasma exposure time.

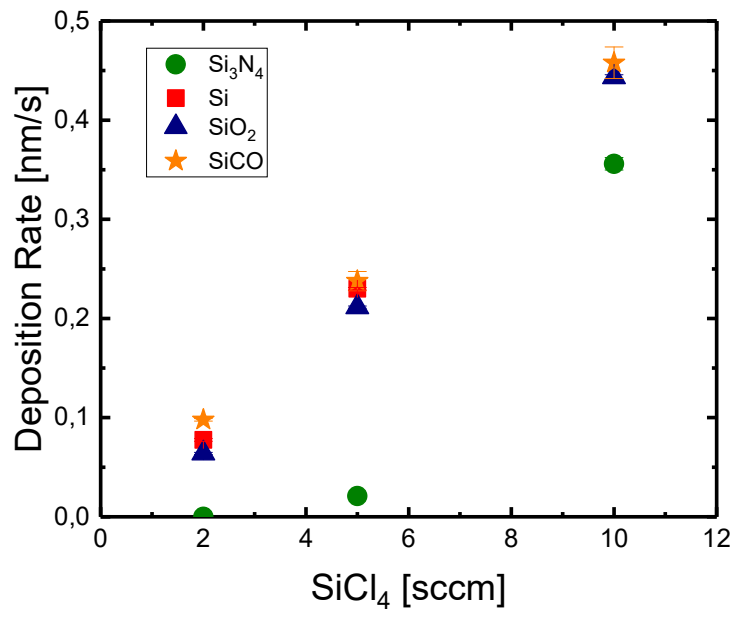
Figure 5 : Take-off angle relative to surface normal dependence of Si2p high-resolution spectra measured on as deposited Si<sub>3</sub>N<sub>4</sub> (a) and after O<sub>2</sub> plasma treatment with no bias (b) or 100 Vb (c).

Figure 6 : Influence of substrate bias voltage on Si<sub>3</sub>N<sub>4</sub> consumption (full dot) or oxide overlayer (open dot) thicknesses. Plasma duration is 60 s. Si<sub>3</sub>N<sub>4</sub> films are deoxidized in HF 1% during 60 s prior running plasma experiments. Inset presents XPS high resolution spectra ( $\theta = 23.75^\circ$ ) of Si2p before (black dashed line) and after plasma processing with 0 V (black), 150 V (red), and 250 V (green) bias voltage.

Figure 7 : Difference of optical emission spectra acquired at 140 and 180 s during plasma processing of a 53 nm thick Si<sub>3</sub>N<sub>4</sub> on 10 nm SiO<sub>2</sub> on Si wafer. The Si<sub>3</sub>N<sub>4</sub> layer is expected to be fully etched after 170 s.

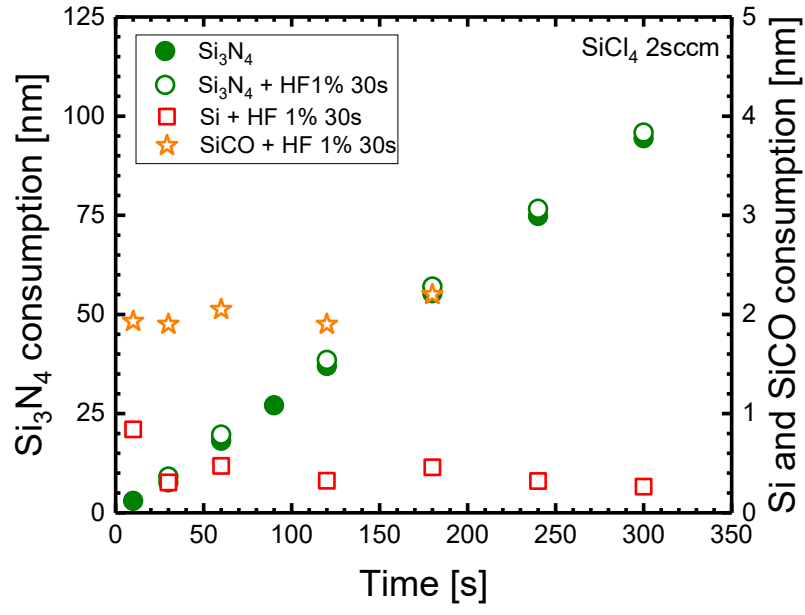
Figure 8 : Time dependence of NH, CN, He, H (divided by 10) and O optical lines intensities (left axis) and substrate power applied to the wafer for 250 bias voltage (right axis) during plasma processing of a 53 nm thick Si<sub>3</sub>N<sub>4</sub> on 10 nm SiO<sub>2</sub> on Si wafer.

This is the author's peer reviewed, accepted manuscript. However, the online version of record will be different from this version once it has been copyedited and typeset.  
PLEASE CITE THIS ARTICLE AS DOI: 10.1116/6.0002434

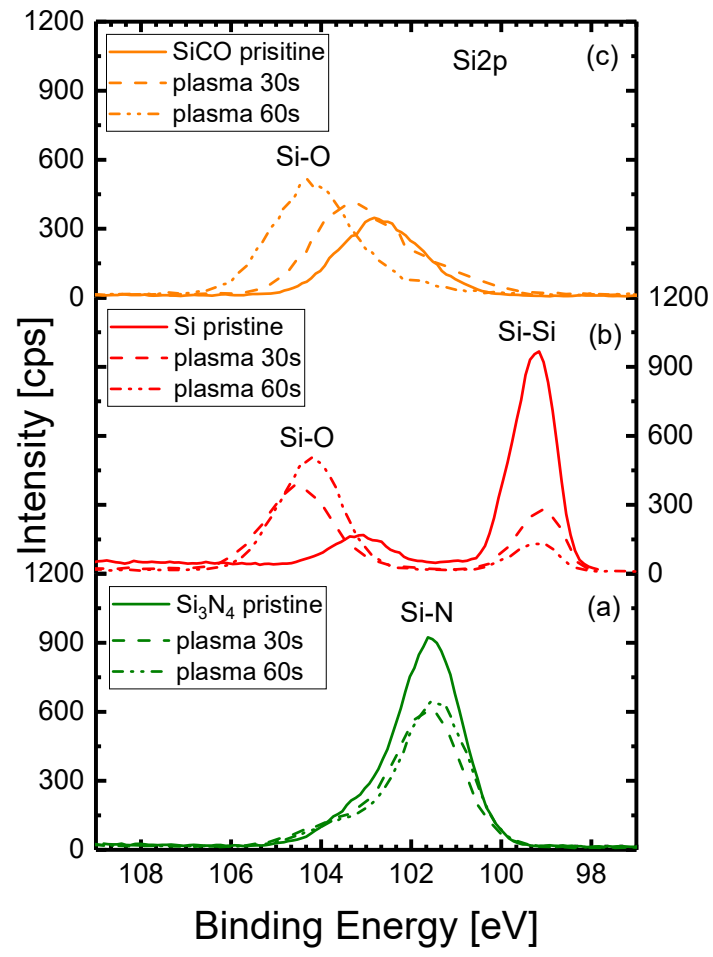


This is the author's peer reviewed, accepted manuscript. However, the online version of record will be different from this version once it has been copyedited and typeset.

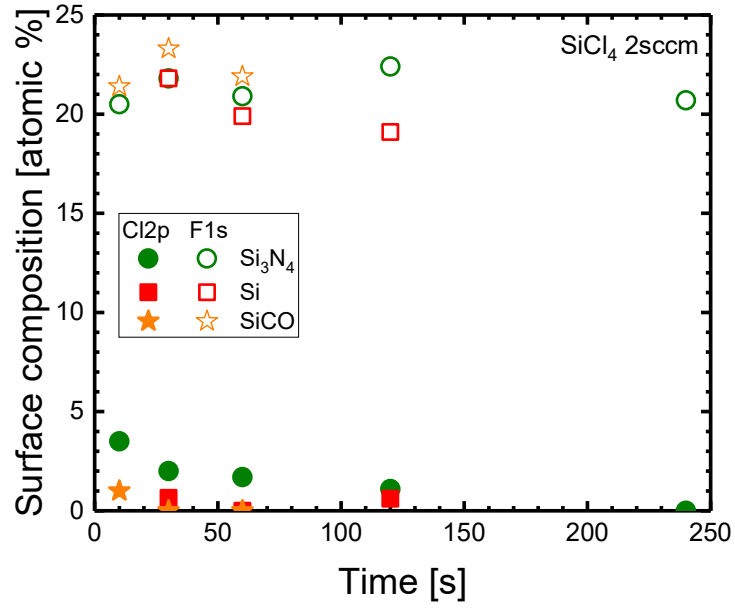
PLEASE CITE THIS ARTICLE AS DOI: 10.1116/1.6.0002434



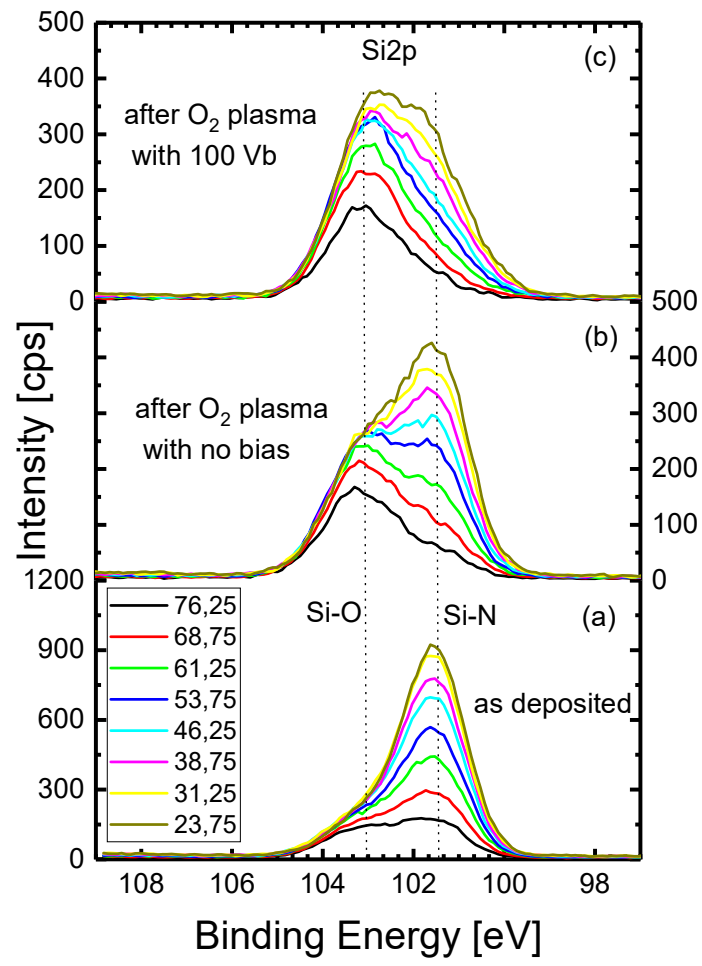
This is the author's peer reviewed, accepted manuscript. However, the online version of record will be different from this version once it has been copyedited and typeset.  
PLEASE CITE THIS ARTICLE AS DOI: 10.1116/1.6.0002434



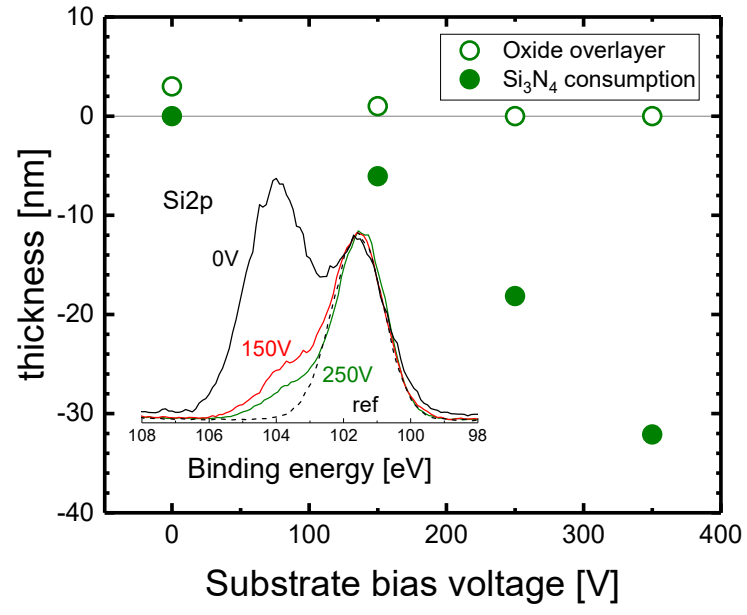
This is the author's peer reviewed, accepted manuscript. However, the online version of record will be different from this version once it has been copyedited and typeset.  
PLEASE CITE THIS ARTICLE AS DOI: 10.1116/6.0002434



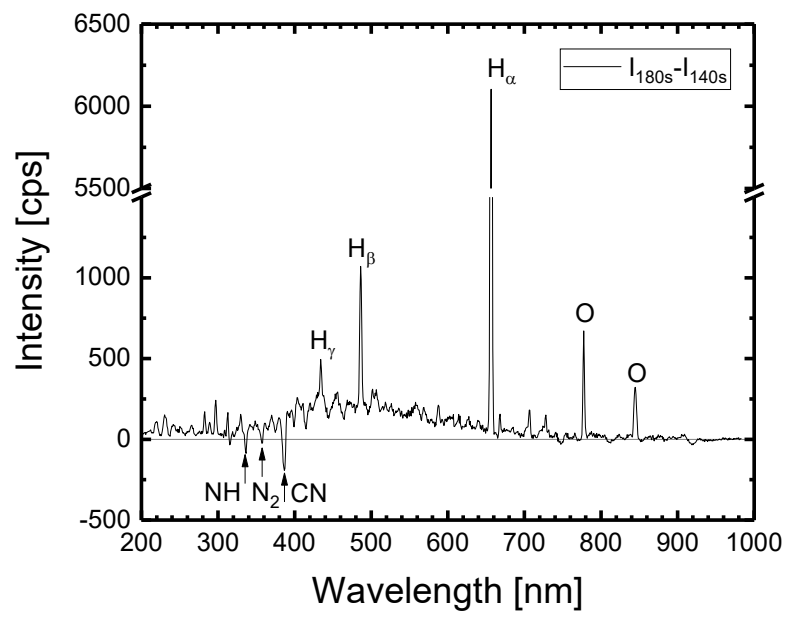
This is the author's peer reviewed, accepted manuscript. However, the online version of record will be different from this version once it has been copyedited and typeset.  
PLEASE CITE THIS ARTICLE AS DOI: 10.1116/1.5002434



This is the author's peer reviewed, accepted manuscript. However, the online version of record will be different from this version once it has been copyedited and typeset.  
PLEASE CITE THIS ARTICLE AS DOI: 10.1116/6.0002434



This is the author's peer reviewed, accepted manuscript. However, the online version of record will be different from this version once it has been copyedited and typeset.  
PLEASE CITE THIS ARTICLE AS DOI: 10.1116/1.5002434



This is the author's peer reviewed, accepted manuscript. However, the online version of record will be different from this version once it has been copyedited and typeset.  
PLEASE CITE THIS ARTICLE AS DOI: 10.1116/1.5002434

